Atmospheric
Measurement
Techniques

Open Access

Discussions

Collection efficiency of the Soot-Particle Aerosol Mass Spectrometer (SP-AMS) for internally mixed particulate black carbon

M. D. Willis[1], A. K. Y. Lee[1], T. B. Onasch[2], E. C. Fortner[2], L. R. Williams[2], A. T. Lambe[2], D. R. Worsnop[2], and J. P. D. Abbatt[1]

[1]Department of Chemistry, University of Toronto, Toronto, Ontario, Canada
[2]Aerodyne Research, Inc., Billerica, Massachusetts, USA

Correspondence to: M. D. Willis (megan.willis@mail.utoronto.ca)
and T. B. Onasch (onasch@aerodyne.com)

Discussion Paper | Discussion Paper | Discussion Paper | Discussion Paper

AMTD

7, 5223–5249, 2014

SP-AMS Collection Efficiency

M. D. Willis et.al.

Title Page

Abstract	Introduction
Conclusions	References
Tables	Figures

|◄ | ►|
◄ | ►
Back | Close

Full Screen / Esc

Printer-friendly Version

Interactive Discussion

Abstract

The soot-particle aerosol mass spectrometer (SP-AMS) uses an intra-cavity infrared laser to vaporize refractory black carbon (rBC) containing particles, making the particle beam–laser beam overlap critical in determining the collection efficiency (CE) for rBC and associated non-refractory particulate matter (NR-PM). This work evaluates the ability of the SP-AMS to quantify rBC and NR-PM mass in internally mixed particles with different thicknesses of organic coating. Using apparent relative ionization efficiencies for uncoated and thickly coated rBC particles, we report measurements of SP-AMS sensitivity to NR-PM and rBC, for Regal Black, the recommended particulate calibration material. Beam width probe (BWP) measurements are used to illustrate an increase in sensitivity for highly coated particles due to narrowing of the particle beam, which enhances the CE of the SP-AMS by increasing the laser beam–particle beam overlap. Assuming complete overlap for thick coatings, we estimate CE for bare Regal Black particles of 0.6 ± 0.1, which suggests that previously measured SP-AMS sensitivities to Regal Black were underestimated by up to a factor of two. The efficacy of the BWP measurements is highlighted by studies at a busy road in downtown Toronto and at a non-roadside location, which show particle beam widths similar to, but greater than that of bare Regal Black and coated Regal Black, respectively. Further BWP measurements at field locations will help to constrain the range of CE for fresh and aged rBC-containing particles. The ability of the SP-AMS to quantitatively assess the composition of internally mixed particles is validated through measurements of laboratory-generated organic coated particles, which demonstrate that the SP-AMS can quantify rBC and NR-PM over a wide range of particle compositions and rBC core sizes.

1 Introduction

Incomplete combustion of fossil fuels, bio-fuels and biomass emit teragram quantities of anthropogenic black carbon to the troposphere every year (Bond et al., 2007, 2013).

Aerosol containing black carbon is an important absorber of shortwave radiation in the atmosphere, with the ability to affect the energy balance at the surface and within the troposphere (Ramanathan and Carmichael, 2008). Black carbon-containing particles are estimated to be the third largest contributor to anthropogenic global warming, after carbon dioxide and methane (Bond et al., 2013). However, the magnitude of their direct effects on radiative balance may become even more significant when black carbon is internally mixed with other aerosol components such as sulphate, nitrate and organic species (Adachi et al., 2010; Jacobson, 2001), though the importance of this enhancement for ambient aerosol remains an open question (Cappa et al., 2012; Lack et al., 2012). The physical and chemical complexity of these particles compound the uncertainty associated with the impacts of black carbon on global and regional climate change and human health (Seinfeld, 2008; Jansen et al., 2005).

A variety of measurement techniques have been used to quantify atmospheric black carbon-containing particles. These include direct techniques, such as the Single Particle Soot Photometer (SP2) that uses laser induced incandescence to quantify refractory black carbon (rBC) and indirect methods using optical techniques, sample combustion, or combustion combined with optical methods (Bond et al., 2013). When aerosols contain a small black carbon mass fraction, reported mass concentrations from a range of measurement techniques can differ significantly (up to 80 %) (Bond et al., 2013). This large range in black carbon mass loadings can be partially attributed to measurement bias, most often for optical methods, associated with the presence of other absorbing species in the aerosol. These measurement uncertainties can make it difficult to understand the spatial and temporal trends and the climate impacts of black carbon.

The Soot-Particle Aerosol Mass Spectrometer (SP-AMS) is a new instrument that combines the SP2 laser system (Schwarz et al., 2010) for volatilization of rBC with the Aerodyne High-Resolution Time-of-Flight AMS (DeCarlo et al., 2006) to quantify non-refractory particulate matter (NR-PM) (Onasch et al., 2012). Near-IR laser vapourization and electron impact ionization facilitate mass spectral detection of light-absorbing rBC and the simultaneous measurement of non-refractory species associated with rBC.

Detection of rBC and NR-PM depends upon the ability of rBC to absorb the IR energy and produce a heating effect significant enough to volatilize the rBC coating material and, upon further heating, the rBC itself. The SP-AMS has been shown to respond linearly and reproducibly to laboratory generated rBC particles (Regal Black (Cabot R400) and flame generated soot) (Onasch et al., 2012). However, in contrast to the Regal Black particles generally used for SP-AMS calibration, freshly emitted particulate black carbon tends to be smaller (e.g., aggregates of $\sim$ 5–50 nm soot spherules, Buseck et al., 2012) and less compact (i.e., lower mass-mobility exponent Cross et al., 2010). Over time these small particles grow and become internally mixed with organic and inorganic species through condensation and coagulation. With ageing, changes in chemical composition and physical properties of rBC particles affect their atmospheric lifetime, radiative properties, and their ability to act as cloud condensation nuclei and as ice nuclei (Liu et al., 2013; Bond et al., 2013). Therefore, it is crucial that the SP-AMS is able to quantify the extent of particle coating and the rBC mass loading. The ability to simultaneously detect rBC and species that condense on it with comparable accuracy is crucial for three reasons; first, to assess the rates at which black carbon processing occurs in the atmosphere; second, to understand the role that such internally mixed particles may play as cloud nuclei; and third, to assess direct effects on solar radiation.

Previous research has applied the linear response of the SP-AMS to measure the size resolved chemical composition of rBC-containing particles during roadside measurements of traffic related pollutants (Massoli et al., 2012), and to characterize rBC mixing state for its relation to black carbon absorption enhancement (Cappa et al., 2012). However, the effect of rBC mixing with NR-PM on the collection efficiency of the SP-AMS laser vapourizer has not been explicitly addressed. In this work, we first examine the effect of rBC-particle coating on the SP-AMS sensitivity to the recommended calibration material, Regal Black. Secondly, we address differences in collection efficiency for bare and internally mixed rBC particles with beam width probe (BWP) measurements to demonstrate particle beam narrowing that occurs due to coating. Finally, using measured sensitivities for laboratory-generated particles, we demonstrate that

SP-AMS Collection Efficiency

M. D. Willis et al.

the SP-AMS can quantify the fraction of rBC in coated particles over a wide range of internally mixed compositions.

2 Experimental

2.1 Particle generation and coating

Experiments were conducted at the University of Toronto (UofT) and at Aerodyne Research, Inc. (ARI) with similar experimental set-ups. A general experimental schematic is shown in Fig. 1. In both cases, rBC containing particles were generated from a water suspension of Regal Black (RB) (Regal 400R Pigment, Cabot Corp.), with concentrations ranging from 10 to 1000 mg L^{-1} in de-ionized water (18 MΩ – cm, TOC < 4 ppb), using a constant output atomizer (TSI Inc., model 3076). The polydisperse aerosol flow was dried with a diffusion drier containing silica gel (< 20 % RH) and directed to a Differential Mobility Analyser (TSI Inc. model 3081) for size selection. The monodisperse aerosol was characterized "bare" (nascent) or after coating with bis(2-ethylhexyl)sebacate (BES) via condensation in a thermally controlled condenser.

The University of Toronto coating apparatus consisted of a 1.3 cm outer diameter, 30 cm long glass tube containing BES. The sample line was connected to the coating region via 0.63 cm diameter glass inlets. The temperature of the coating region was controlled using heating tape, monitored using a thermocouple and varied from room temperature up to 125 °C. Aerosol carrier flow through the coating region was 450 cm^3 min^{-1}. The ARI coating apparatus consisted of a 60 cm long, 1.3 cm outer diameter glass tube wrapped in heating tape and temperature controlled using an Omega PID controller and a thermocouple. The tube has two temperature zones (∼ 30 cm each) and was operated with the downstream zone set to ∼ 20 °C less than the upstream zone. The temperature of the upstream zone was varied from room temperature to 150 °C. The flow through the coating tube was 750 cm^3 min^{-1}.

SP-AMS Collection Efficiency

M. D. Willis et.al.

Title Page

Abstract	Introduction
Conclusions	References
Tables	Figures

|◄ | ►|

◄ | ►

Back | Close

Full Screen / Esc

Printer-friendly Version

Interactive Discussion

2.2 Particle characterization

The size selected bare and coated rBC particles were characterized for particle mass using a mass analyzer (Aerosol Particle Mass Analyzer (APM model 3600, Kanomax Inc.) or Centrifugal Particle Mass Analyzer (CPMA, Cambustion), Olfert and Collings, 2005), number concentration using a Condensation Particle Counter (CPC, TSI Inc., model 3776 and 3022a), and contributions from doubly charged particles using a Scanning Mobility Particle Sizer (SMPS. TSI Inc., model 3936). Particle number concentration was monitored before and after coating, and used to monitor particle loss or homogeneous nucleation. The mass analyzer was scanned using both the rotational speed and voltage to measure the size resolved mass distribution for coated and bare particles. From the mass analyzer measurements of bare and coated Regal black particles we define the mass ratio of organic coating to Regal Black ($R_{Org/RB} = mass_{BES}/mass_{RB}$) and the mass fraction of Regal Black ($f_{RB} = mass_{RB}/(mass_{BES} + mass_{RB})$), where $mass_{BES} = mass_{RB,coated} - mass_{RB}$.

2.3 The Soot-Particle Aerosol Mass Spectrometer (SP-AMS)

The Soot-Particle Aerosol Mass Spectrometer (SP-AMS) is an Aerodyne High-Resolution AMS equipped with an infrared laser vapourization module similar to that of the Single Particle Soot Photometer (Droplet Measurement Technologies) as described in detail by Onasch et al. (2012). In brief, the SP-AMS laser vapourization module uses a continuous wave intra-cavity 1064 nm Nd:YAG laser, situated perpendicular to the particle beam, that allows vapourization and subsequent detection of refractory black carbon (rBC) species (Onasch et al., 2012). The width of the laser beam (fundamental transverse mode, TEM00, with Gaussian profile) is dictated by the length of the lasing cavity and the curvature of the optics, which are fixed in SP-AMS instruments. Particles are focused with an aerodynamic lens into a narrow beam which crosses the IR laser beam. Particles containing rBC absorb IR energy and are heated, first vaporizing non-refractory (NR) coatings (estimated temperature < 600 °C) and then vaporizing the rBC

(estimated temperature $\sim 4000\,°C$ Onasch et al., 2012). Neutral gas phase analytes are ionized using 70 eV electron impact ionization. Three SP-AMS instruments were used in this study (UofT SN 215-121, ARI SN 215-039 and 215-130), all of which were operated in V-ToF mode with both the tungsten vapourizer ($\sim 600\,°C$) and the laser vapourizer simultaneously, unless otherwise noted.

Particle beam alignment with the tungsten vapourizer and the IR laser beam was confirmed preceding these experiments and IR laser power was optimized for saturation of the rBC signal. The physical distance between the center of the tungsten vapourizer and the vertical position of maximum sensitivity for Regal Black in the IR laser was ≤ 0.5 mm. Data acquisition alternated between mass spectrum (MS) and particle time-of-flight (pToF) modes. Data were analyzed using the AMS analysis software Squirrel version 1.51H and Pika version 1.10H. Signals of rBC from Regal Black were quantified by the sum of C_1^+ to C_9^+ peaks, using high resolution ($R \approx 1900$–2100) MS data. The average ratio of C_1^+ to C_3^+ (0.6), obtained from bare Regal Black, was used to correct the C_1^+ peak intensity for interference from non-refractory species in coated particles. The signals arising from refractory CO^+ and CO_2^+ (Corbin et al., 2013) were not included in the organic loading if it accounted for greater than 10 % of the total organic signal, since the appropriate chemical fragmentation of these species arising from Regal Black was not quantified in this work.

For comparison to mass analyzer derived mass fractions of Regal black (f_{RB}) in coated particles, chemical identification and quantification was carried with each SP-AMS instrument. The SP-AMS derived f_{RB} (or $R_{Org/RB}$) was determined through quantification of rBC and coating, taking into account NR-PM already present on Regal black as follows:

$$f_{RB} = \frac{mass_{rBC} + mass_{Org,\,RB}}{mass_{rBC} + mass_{Org,\,RB} + mass_{BES}} \tag{1}$$

where $mass_{Org,\,RB}$ is the mass of organic species present on Regal black.

2.4 Particle beam width measurements

Each SP-AMS was equipped with a beam width probe (BWP) consisting of a vertical wire of 0.46 mm or 0.41 mm in width (UofT and ARI, respectively). The BWP wire was oriented perpendicular to the laser beam axis and stepped across the particle beam parallel to the laser axis (horizontally). As detailed in Huffman et al. (2005), the BWP wire blocks a fraction of sampled particles from reaching the vapourizer at each given step. By analyzing the results from multiple wire steps across the particle beam, the particle beam divergence can be determined. In the horizontal orientation, the laser beam produces uniform vapourization of rBC, thus allowing direct measurement of rBC particle beam widths. Particle beam widths (σ) in this work are determined by fitting a one dimensional Gaussian profile to the measured transmission profile as a function of the distance the BWP wire travels along the horizontal axis of the laser beam. These widths are slightly different widths than those derived by Huffman et al. (2005), where a two dimensional Gaussian profile was assumed for the particle beam and the tungsten vapourizer geometry was explicitly included in their modelling. BWP measurements were also carried out by rotating the BWP such that the wire was oriented parallel to the laser beam axis and could be stepped across the particle beam perpendicular to the laser beam (vertically). Measurements in this orientation can provide some insight into the effective laser beam width for rBC. Note that the UofT SP-AMS was operated without the tungsten vapourizer during these vertical BWP measurements. See Fig. S1 for an illustration of BWP orientation for particle and laser beam width measurements.

3 Results and discussion

3.1 The effect of rBC-particle coating on SP-AMS collection efficiency

3.1.1 SP-AMS calibration

The goal of this section is to examine the effect of rBC mixing state on SP-AMS sensitivity to rBC and associated NR-PM. To do so, we measure the apparent ionization efficiency of rBC and organic coating material relative to nitrate ($RIE_{rBC,\,app}$ and $RIE_{Org,\,app}$) for a variety of particle coating thicknesses and compare these observations to uncoated values. The relative ionization efficiency, defined in previous work (Jimenez et al., 2003; Onasch et al., 2012), is applied to quantify the mass concentration of a particulate species. Using the mass based ionization efficiency for nitrate (mIE_{NO_3}, in units of ions per picogram) the mass concentration of species "s" can be determined as follows:

$$C_s = \frac{1}{CE_s \cdot RIE_s \cdot mIE_{NO_3} \cdot Q} \sum_i I_{s,\,i} \tag{2}$$

where C_s is the mass concentration of species "s," $RIE_s = mIE_s/mIE_{NO_3}$, Q is the flow rate, CE_s is the species specific collection efficiency, and each $I_{s,\,i}$ is an ion signal associated with species "s." The apparent mass based ionization efficiency is dependent on the collection efficiency (i.e., $RIE_{s,\,app} = RIE_s \cdot CE_s$) for the particular particle type, which is given by the product of terms associated with loss due to the aerodynamic lens (E_L), beam divergence (E_S), and particle bounce (E_B) off of the tungsten vapourizer ($CE = E_L \cdot E_S \cdot E_B$) (Huffman et al., 2005). For particles with unit lens transmission, the most important loss mechanism when considering the laser vapourization module of the SP-AMS is beam divergence, such that $CE \cong E_S$ (Onasch et al., 2012).

$RIE_{rBC,\,app}$ and $RIE_{Org,\,app}$ values were determined from independent measurements of $mIE_{rBC,\,app}$, $mIE_{Org,\,app}$ and mIE_{NO_3}. $mIE_{rBC,\,app}$ values were measured with monodisperse rBC containing particles (Regal Black, final vacuum aerodynamic diameter (d_{va})

200–500 nm for a range of coating thicknesses) that were characterized in terms of their per particle mass and number concentration. Particles with 300–500 nm mobility diameter were used to ensure unit lens transmission ($E_L = 1$). Good agreement was observed between $RIE_{rBC, app}$ values obtained from bare Regal Black over the particle size range of 250–400 nm, which suggests minimal difference in collection efficiency for these uncoated particles.

3.1.2 The effect of rBC-particle coating

$RIE_{rBC, app}$ and $RIE_{Org, app}$ values were measured over a range of BES coating thicknesses, with the mass ratio of BES to Regal Black ($R_{Org/RB}$) ranging from 0 to 6 (corresponding to a mass fraction of Regal Black, f_{RB}, ranging from 1 to 0.15). Figure 2a demonstrates that as $R_{Org/RB}$ increases, the apparent sensitivity to rBC increases by approximately a factor of two, for two SP-AMS instruments, and seems to saturate at $R_{Org/RB} > 3$. A similar trend is shown in Fig. 2b for the BES coating from each SP-AMS instrument. A comparable increase in sensitivity with particle coating was also observed with a third SP-AMS instrument (see Fig. S2); however, particle mass analyzer measurements were not available during this experiment so the data were not included in Fig. 2. The difference in sensitivity enhancement evident in Fig. 2a between the two instruments could be due to differences in the final coated particle size or to differences in the uniformity of particle coating provided by each coating apparatus, both of which could result in differences in particle focusing in the aerodynamic lens and the resulting particle beam–laser beam overlap. The possibility of homogeneously nucleated organic particles, which cannot be neglected in these experiments, could also lead to differences in the overall RIE enhancement.

The relatively large values of $RIE_{Org, app}$ observed in this work for BES were higher than the recommended value of 1.4 for all sampled organics from ambient sources (Alfarra et al., 2004). As noted in Jimenez et al. (2003) individual organic molecules may exhibit different RIE values, including values greater than 1.4. Utilizing the results published in Jimenez et al. (2003) (Fig. 6), organic hydrocarbon compounds have an

Title Page

Abstract | Introduction

Conclusions | References

Tables | Figures

◄ | ►|

◄ | ►

Back | Close

Full Screen / Esc

Printer-friendly Version

Interactive Discussion

apparently higher RIE than highly oxygenated organic compounds (RIE ~ 2 for hydrocarbons vs. ~ 1.3 for oxygenated compounds). BES has a relatively low O : C ratio ($4 : 26 \cong 0.15$), and thus may exhibit an RIE similar to hydrocarbons up to ~ 2. For these data, the apparent RIE (defined as SP-AMS measured ions divided by the difference of the coated to uncoated per particle mass from the mass analyzer) measured for BES under thin coating conditions are highly uncertain due to the difference term in the denominator, which goes to zero with thin coatings. Under thicker coating conditions, the observed $RIE_{Org, app}$ values are significantly higher than 2. Reasons for this discrepancy may be due to differences between the laser and heated tungsten vaporizers and may include; (1) an enhanced ionization efficiency for gas phase molecules generated in the laser vapourizer due to their position relative to the filament; (2) an improved ion extraction efficiency of ions originating from neutral gas-phase molecules vapourized at the laser vapourizer, due to their position in the ion chamber; or (3) a collection efficiency on the tungsten vapourizer of less than one for organics in rBC particles. The fact that an increased sensitivity to NR-PM is observed not only with dual vapourizers, but also with the laser vapourizer only may suggest an enhanced sensitivity to species vapourized from the laser vapourizer compared with the same species vapourized from to the tungsten vapourizer.

The observed dependence of SP-AMS sensitivity on particle coating thickness (Fig. 2) is likely caused by decreased particle beam divergence with coating, resulting in greater laser–particle beam overlap. The saturation behaviour shown in Fig. 2 can be used to estimate collection efficiency (E_S) for bare Regal Black particles and for the organic species on thinly coated Regal Black particles. With the assumption that the sensitivity measured at saturation (i.e., highly coated particles) corresponds to complete particle beam–laser beam overlap ($E_S = 1$ and $RIE_{rBC, app} = RIE_{rBC}$), then E_S can be inferred by dividing $RIE_{rBC, app}$ ($RIE_{Org, app}$) values for the bare (nascent) Regal black by the average maximum value observed in each instrument for coated particles ($RIE_{rBC, app}$ and $RIE_{Org, app}$). From the data sets presented in Fig. 2, for bare (nascent) Regal black, an E_S value of 0.6 ± 0.1 was determined. This result indicates

that Regal Black calibrations used in the past, with mIE_{rBC} of ~ 150 ± 25 ions pg^{-1} and corresponding RIE_{rBC} of 0.2 ± 0.1 (Onasch et al., 2012), are underestimated by approximately a factor of two.

3.2 rBC Particle beam divergence

In this section, the impact of particle coating on SP-AMS collection efficiency is explored using particle beam width measurements. Non-spherical particles produce more divergent particle beams compared to spherical particles, owing to lift and drag on irregularly shaped particles. As non-spherical rBC-containing particles are coated with a liquid organic species, they become more spherical in shape (e.g., Cross et al., 2010). Therefore, a change in rBC-containing particle shape could affect particle beam divergence enough to alter the extent of particle beam–laser beam overlap, thus altering the collection efficiency (E_s). To investigate this difference in sensitivity with particle coating, the change in particle beam width was measured as a function of coating thickness with a beam width probe (BWP).

In this context, signal transmission is defined as the signal intensity at a given BWP position relative to that of an unblocked beam, normalized to particle number concentration. A decreasing signal transmission with a BWP centered in the particle beam is indicative of particle beam narrowing. Figure 3 compares signal transmission vs. BWP position curves for 200 nm uncoated Regal Black, BES coated Regal Black particles ($R_{Org/RB} \cong 3$) and 300 nm ammonium nitrate (as an example of a well focused beam), each fit to a 1-D Gaussian distribution. The standard deviation (σ) of this distribution is used to describe the particle beam width (i.e., 4σ, or $\pm 2\sigma$, defines 95.4 % of the particle beam width). As shown in Table 1 BWP measurements indicate that the particle beam narrows from $\sigma \sim 0.4$ mm for bare, 200 and 300 nm Regal black particles to approximately 0.1–0.2 mm (ARI and UofT measurements, respectively) when the particles are coated with BES ($R_{Org/RB} \sim 3$). The differences in beam width measured in the two experiments likely arise from differences in the final coated particle size ($\cong 375$ nm and

$d_{va} \cong 280\,nm$, see Table 1). The beam width for these coated Regal Black particles approaches that of pure 230 nm BES particles ($\sigma = 0.12\,mm$) (Huffman et al., 2005). However, it should be noted that 1-D Gaussian fits to BWP curves at low σ (i.e., a well focused beam) may overestimate the particle beam width (Huffman et al., 2005).

5   Figure 4a demonstrates the relationship between sensitivity to rBC, particle beam width and coating thickness. With a BWP centered in the Regal Black particle beam, signal transmission decreases as $R_{Org/RB}$ increases (i.e., the particle beam width decreases as coating thickness increases). Furthermore, with the BWP positioned outside of the particle beam, $mIE_{rBC,\,app}$ increases as $R_{Org/RB}$ increases. These two observations suggest that as rBC particles become more coated the particle beam–laser beam overlap becomes more complete, giving rise to enhanced signal intensity for rBC and the associated NR-PM. RIE_{app} vs. SP-AMS derived $R_{Org/RB}$ plots for this data set, similar to those in Fig. 2, are presented in Fig. S2. Figure 4b demonstrates that rBC and organic signal transmission both decrease due to particle coating, with an approximately one-to-one relationship.

3.3   Measure of effective laser width for rBC

To aide in assessing the importance of incomplete laser beam–particle beam overlap for SP-AMS quantification of rBC an upper limit for the effective laser beam width was estimated, and compared to ambient particle beam-width measurements.

20   When the SP-AMS is operated without the tungsten vapourizer and the BWP is positioned such that the wire could be moved vertically (perpendicular to the laser beam axis), some information can be gained about the effective width of the laser beam in much the same manner as is done for particle beam widths. Since the resulting BWP position vs. signal transmission curve is affected not only by the true laser beam effective width but also by the particle beam and the BWP wire width, these measurements only allow for estimation of an upper limit for the effective SP-laser width for rBC. Figure 5 demonstrates that with a 0.46 mm BWP centered in front of the IR laser an average of $97 \pm 2\,\%$ of the rBC signal was attenuated. From this information and the

SP-AMS Collection Efficiency

M. D. Willis et.al.

Title Page

Abstract | Introduction

Conclusions | References

Tables | Figures

|◄ | ►|

◄ | ►

Back | Close

Full Screen / Esc

Printer-friendly Version

Interactive Discussion

projected BWP wire width (see Fig. 5) the effective laser beam width (4σ) can be es-
timated as less than 0.73 mm. Therefore, the effective laser beam width (σ) is at most
0.18 mm. The narrowness of the effective laser beam width highlights the importance
of determining E_S for accurate quantification of rBC mass loadings. Further measure-
ments are required to unambiguously determine the effective IR laser beam width.

3.4 Ambient particle beam width measurements

Beam width probe measurements of ambient rBC-containing particles provide insight
into the morphology, and collection efficiency, of these particles. Ambient rBC particles
sampled at 5 m height and 16 m from a roadside in downtown Toronto gave wider
particle beams compared to those sampled away from large roadways, suggesting
that fresh rBC emissions produce more divergent beams, and that particle processing
reduces particle beam divergence (see Table 1). Both ambient BWP measurements
indicated beam widths narrower than that of flame soot ($\sigma = 0.77$ mm) (Huffman et al.,
2005), and fall within the range of ambient particle beam widths observed by Salcedo
et al. (2007).

The similarity in beam width for the "fresh" rBC-particles measured here and the
beam width for bare Regal Black could suggest similar collection efficiencies for these
types of particles. However, previous comparisons of SP-AMS rBC mass loadings
with those derived from other instruments, such as the Multiangle Absorption Pho-
tometer (MAAP), have suggested lower overall collection efficiencies for ambient rBC-
containing particles (i.e., 0.1 to 0.3) (Massoli et al., 2012; Dallmann et al., 2014). Future
ambient BWP measurements, in conjunction with comparison to other instruments, will
further constrain the SP-AMS collection efficiency for ambient rBC and NR-PM.

Comparison of the estimated upper limit of laser beam width ($\sigma \leq 0.18$ mm) with
ambient and laboratory particle beam width measurements highlights the relevance of
incomplete beam overlap for SP-AMS quantification. It is important to note that this
overlap mismatch is only relevant in the dimension perpendicular to the IR laser, such

that a simple comparison of particle and laser beam widths is insufficient to provide a quantitative estimate of collection efficiency.

3.5 Quantification of rBC mixing state in organic coated particles

In order to quantify mixing state in terms of the mass fraction of rBC present in ambient aerosol the SP-AMS must be operated without the tungsten vapourizer to avoid interference from externally mixed NR-PM; however, in laboratory experiments when all particles are known to contain rBC such a quantification is possible. In this section, the ability of the SP-AMS to quantify mixing state for laboratory-generated internally mixed rBC particles is examined. It is important to note that these experiments focused on liquid organic coatings, which are similar to hydrocarbon-like organic coatings but may not resemble more oxygenated organic coatings.

To accurately quantify rBC and NR-PM simultaneously from the same particles, it is important that the effective IR laser beam width for vapourizing all particle phase species is similar. If, for example, NR-PM could be vapourized in lower energy regions of the IR laser (i.e., at the edges of the beam) that do not effectively vapourize rBC, NR-PM would have a wider effective laser beam width. In such a case, the contribution of organic species to the overall particulate mass loading could be overestimated relative to rBC for $E_S < 1$. Figure 4b demonstrates that the rBC and the organic signal transmission decrease with coating thickness in a similar manner when a BWP is placed in the center of the particle beam. Furthermore, Fig. 2 demonstrates similar increases in RIE_{rBC} and RIE_{Org} with coating. Overall, these observations suggest that the effective IR laser beam width, in terms of its ability to vapourize different particle phase species, is similar for rBC and BES.

To further assess the ability of the SP-AMS to quantify the mixing state of rBC-containing particles the mass fraction of Regal Black ($f_{RB} = mass_{RB}/(mass_{BES} + mass_{RB})$) in BES coated particles of various rBC core sizes (40 to 300 nm) was measured with the SP-AMS and compared to f_{RB} obtained from particle mass measurements. The mass analyzer characterized coating thickness by the difference between

Title Page

Abstract | Introduction

Conclusions | References

Tables | Figures

◄◄ | ►►

◄ | ►

Back | Close

Full Screen / Esc

Printer-friendly Version

Interactive Discussion

average particle mass before and after coating. Since the mass analyzer measures the total mass of Regal Black particles (i.e., rBC and associated organic species on Regal Black), the f_{RB} measured by the SP-AMS was calculated by including the contribution from organics present on the particles prior to coating. Figure 6 demonstrates that f_{RB} values derived from the SP-AMS agree well with f_{RB} values from particle mass measurements when SP-AMS values are corrected for CE and sensitivity effects. SP-AMS values using the standard RIE_{rBC} and RIE_{Org} (i.e., 0.2 and 1.4, respectively) can underestimate f_{RB} by up to $\sim 50\%$ and the data in Fig. 6 exhibit a pronounced non-linear relationship. For the specific case of BES, if the RIE_{Org} value is higher than the recommended value of 1.4, the underestimation would be less than that depicted in Fig. 6. To obtain the corrected values, the upward trend in RIE_{app} for rBC and NR-PM with increasing coating thickness (Fig. 2) was fit to a sigmoid relationship to obtain the appropriate values for a given coating thickness. When the changes in CE with particle coating are taken into account the relationship in Fig. 6 shows excellent linearity ($R^2 = 0.98$, slope $= 1.01 \pm 0.05$).

These results indicate that the SP-AMS can accurately measure the fraction of Regal Black in laboratory generated organic coated particles, down to f_{RB} of ~ 0.05 for small (i.e., 40 nm) inclusions, when instrumental sensitivity is well known. The ability of the SP-AMS to quantitatively characterize rBC mixing state depends strongly upon the $RIE_{rBC, app}$ and $RIE_{Org, app}$ values used to calculate particulate mass loadings. In addition, knowledge of the value of E_S, or particle loss owing to beam divergence, is essential for quantitative SP-AMS measurements of mixing state.

4 Summary

Our results demonstrate that particle morphology affects the SP-AMS particle beam width, which in turn affects the collection efficiency through the overlap of the particle beam and the laser beam. Observations from laboratory-generated internally mixed rBC-containing particles in three SP-AMS instruments indicate that particle coating

influences CE through beam divergence (E_S). We estimate CE for bare Regal Black particles, the recommended calibration material, to be 0.6 ± 0.1 suggesting that previous rBC calibrations of the SP-AMS with Regal Black were underestimated by up to a factor of two. CE for ambient rBC-containing particles will depend on their morphology and the resulting particle-beam width, which is largely unconstrained.

Ambient BWP measurements indicate that fresh rBC containing particles sampled at the roadside in downtown Toronto have particle beam widths similar to, but greater than, bare Regal Black, and thus likely a collection efficiency less than bare Regal Black. More processed rBC particles have a smaller beam width and therefore a larger value of CE. The importance of measuring E_S is further highlighted by the upper limit estimate of the effective laser beam width for rBC, from BWP measurements, of $\sigma \leq 0.18$ mm. Further work is required to provide an unambiguous measurement of the IR laser beam width, which could be applied in conjunction with ambient particle beam width measurements to provide a more specific estimate of CE in different sampling environments by relation to particle beam width.

This work demonstrates for the first time the ability of the SP-AMS to quantitatively characterize the levels of internally mixed particulate rBC and NR-PM in laboratory-generated particles over a wide range of compositions, when instrumental sensitivity is well known. In particular, the SP-AMS can quantify the rBC mixing state even for highly organic-rich particles ($f_{RB} < 0.05$) with atmospherically relevant rBC core sizes (i.e., ≥ 40 nm mobility diameter). The quantitative capability of the SP-AMS, combined with its ability to chemically characterize NR-PM coated on rBC-particles, can provide unique insight into the characteristics of ambient black carbon.

The Supplement related to this article is available online at doi:10.5194/amtd-7-5223-2014-supplement.

References

Adachi, K., Chung, S. H., and Buseck, P. R.: Shapes of soot aerosol particles and implications for their effects on climate, J. Geophys. Res.-Atmos., 115, D15206, doi:10.1029/2009JD012868, 2010. 5225

Alfarra, M. R., Coe, H., Allan, J. D., Bower, K., Boudries, H., Canagaratna, M. R., Jimenez, J. L., Jayne, J. T., Garforth, A., Li, S. M., and Worsnop, D. R.: Characterization of urban and rural organic particulate in the Lower Fraser Valley using two Aerodyne Aerosol Mass Spectrometers, Atmos. Environ., 38, 5745–5758, 2004. 5232

Bond, T. C., Bhardwaj, E., Dong, R., Jogani, R., Jung, S. K., Roden, C., Streets, D. G., and Trautmann, N. M.: Historical emissions of black and organic carbon aerosol from energy-related combustion, 1850–2000, Global Biogeochem. Cy., 21, GB2018, doi:10.1029/2006gb002840, 2007. 5224

Bond, T. C., Doherty, S. J., Fahey, D. W., Forster, P. M., Berntsen, T., DeAngelo, B. J., Flanner, M. G., Ghan, S., Kärcher, B., Koch, D., Kinne, S., Kondo, Y., Quinn, P. K., Sarofim, M. C., Schultz, M. G., Schulz, M., Venkataraman, C., Zhang, H., Zhang, S., Bellouin, N., Guttikunda, S. K., Hopke, P. K., Jacobson, M. Z., Kaiser, J. W., Klimont, Z., Lohmann, U., Schwarz, J. P., Shindell, D., Storelvmo, T., Warren, S. G., and Zender, C. S.: Bounding the role of black carbon in the climate system: a scientific assessment, J. Geophys. Res.-Atmos., 118, 5380–5552, doi:10.1002/jgrd.50171, 2013. 5224, 5225, 5226

Buseck, P. R., Adachi, K., Gelencsér, A., Tompa, É., and Pósfai, M.: Are black carbon and soot the same?, Atmos. Chem. Phys. Discuss., 12, 24821–24846, doi:10.5194/acpd-12-24821-2012, 2012. 5226

Cappa, C. D., Onasch, T. B., Massoli, P., Worsnop, D. R., Bates, T. S., Cross, E. S., Davidovits, P., Hakala, J., Hayden, K. L., Jobson, B. T., Kolesar, K. R., Lack, D. A., Lerner, B. M., Li, S. M., Mellon, D., Nuaaman, I., Olfert, J. S., Petaja, T., Quinn, P. K., Song, C., Subramanian, R., Williams, E. J., and Zaveri, R. A.: Radiative absorption enhancements due to the mixing state of atmospheric black carbon, Science, 337, 1078–1081, 2012. 5225, 5226

SP-AMS Collection Efficiency

M. D. Willis et.al.

Title Page	
Abstract	Introduction
Conclusions	References
Tables	Figures
|◄	►|
◄	►
Back	Close
Full Screen / Esc	
Printer-friendly Version	
Interactive Discussion	

Corbin, J. C., Sierau, B., Gysel, M., Laborde, M., Keller, A., Kim, J., Petzold, A., Onasch, T. B., Lohmann, U., and Mensah, A. A.: Mass spectrometry of refractory black carbon particles from six sources: carbon-cluster and oxygenated ions, Atmos. Chem. Phys., 14, 2591–2603, doi:10.5194/acp-14-2591-2014, 2014. 5229

5 Cross, E. S., Onasch, T. B., Ahern, A., Wrobel, W., Slowik, J. G., Olfert, J., Lack, D. A., Massoli, P., Cappa, C. D., Schwarz, J. P., Spackman, J. R., Fahey, D. W., Sedlacek, A., Trimborn, A., Jayne, J. T., Freedman, A., Williams, L. R., Ng, N. L., Mazzoleni, C., Dubey, M., Brem, B., Kok, G., Subramanian, R., Freitag, S., Clarke, A., Thornhill, D., Marr, L. C., Kolb, C. E., Worsnop, D. R., and Davidovits, P.: Soot particle studies – instrument intercomparison – project overview, Aerosol Sci. Tech., 44, 592–611, 2010. 5226, 5234

Dallmann, T., Onasch, T. B., T. W., K., Worton, D., Fortner, E. C., S. C., H., Wood, E., Franklin, J., Worsnop, D. R., Goldstein, A., and Harley, R.: Characterization of particulate matter emissions form on-road gasoline and diesel vehicles using a soot particle aerosol mass spectrometer, Atmos. Chem. Phys. Discuss., 14, 4007–4049, 2014,
15 http://www.atmos-chem-phys-discuss.net/14/4007/2014/. 5236

DeCarlo, P. F., Kimmel, J. R., Trimborn, A., Northway, M. J., Jayne, J. T., Aiken, A. C., Gonin, M., Fuhrer, K., Horvath, T., Docherty, K. S., Worsnop, D. R., and Jimenez, J. L.: Field-deployable, high-resolution, time-of-flight aerosol mass spectrometer, Anal. Chem., 78, 8281–8289, 2006. 5225

20 Huffman, J., Jayne, J. T., Drewnick, F., Aiken, A. C., Onasch, T. B., Worsnop, D. R., and Jimenez, J.: Design, modeling, optimization, and experimental tests of a particle beam width probe for the aerodyne aerosol mass spectrometer, Aerosol Sci. Tech., 39, 1143–1163, 2005. 5230, 5231, 5235, 5236, 5243

Jacobson, M. Z.: Strong radiative heating due to the mixing state of black carbon in atmospheric
25 aerosols, Nature, 409, 695–697, 2001. 5225

Jansen, K. L., Larson, T. V., Koenig, J. Q., Mar, T. F., Fields, C., Stewart, J., and Lippmann, M.: Associations between health effects and particulate matter and black carbon in subjects with respiratory disease, Environ. Health Persp., 113, 1741–1746, 2005. 5225

Jimenez, J. L., Jayne, J. T., Shi, Q., Kolb, C. E., Worsnop, D. R., Yourshaw, I., Seinfeld, J. H.,
30 Flagan, R. C., Zhang, X. F., Smith, K. A., Morris, J. W., and Davidovits, P.: Ambient aerosol sampling using the Aerodyne Aerosol Mass Spectrometer, J. Geophys. Res.-Atmos., 108, 8425, doi:10.1029/2001jd001213, 2003. 5231, 5232

SP-AMS Collection Efficiency

M. D. Willis et.al.

Title Page

Abstract | Introduction

Conclusions | References

Tables | Figures

◄ | ►

Back | Close

Full Screen / Esc

Printer-friendly Version

Interactive Discussion

Lack, D. A., Langridge, J., Bahreini, R., Cappa, C., Middlebrook, A., and Schwarz, J. P.: Brown carbon and internal mixing in biomass burning particles, P. Natl. Acad. Sci. USA, 109, 14802–14807, doi:10.1073/pnas.1206575109, 2015–2029, 2012. 5225

Liu, D., Allan, J., Whitehead, J., Young, D., Flynn, M., Coe, H., McFiggans, G., Fleming, Z. L., and Bandy, B.: Ambient black carbon particle hygroscopic properties controlled by mixing state and composition, Atmos. Chem. Phys., 13, 2015–2029, doi:10.5194/acp-13-2015-2013, 2013. 5226

Massoli, P., Fortner, E. C., Canagaratna, M. R., Williams, L. R., Zhang, Q., Sun, Y., Schwab, J. J., Trimborn, A., Onasch, T. B., Demerjian, K. L., Kolb, C. E., Worsnop, D. R., and Jayne, J. T.: Pollution gradients and chemical characterization of particulate matter from vehicular traffic near major roadways: results from the 2009 queens college air quality study in NYC, Aerosol Sci. Tech., 46, 1201–1218, 2012. 5226, 5236

Olfert, J. S. and Collings, N.: New method for particle mass classification – the couette centrifugal particle mass anlayzer, J. Aerosol Sci., 36, 1338–1352, 2005. 5228

Onasch, T. B., Trimborn, A., Fortner, E. C., Jayne, J. T., Kok, G. L., Williams, L. R., Davidovits, P., and Worsnop, D. R.: Soot particle aerosol mass spectrometer: development, validation, and initial application, Aerosol Sci. Tech., 46, 804–817, 2012. 5225, 5226, 5228, 5229, 5231, 5234

Ramanathan, V. and Carmichael, G.: Global and regional climate changes due to black carbon, Nat. Geosci., 1, 221–227, 2008. 5225

Salcedo, D., Onasch, T. B., Canagaratna, M. R., Dzepina, K., Huffman, J. A., Jayne, J. T., Worsnop, D. R., Kolb, C. E., Weimer, S., Drewnick, F., Allan, J. D., Delia, A. E., and Jimenez, J. L.: Technical Note: Use of a beam width probe in an Aerosol Mass Spectrometer to monitor particle collection efficiency in the field, Atmos. Chem. Phys., 7, 549–556, doi:10.5194/acp-7-549-2007, 2007. 5236

Schwarz, J. P., Spackman, J. R., Gao, R. S., Perring, A. E., Cross, E., Onasch, T. B., Ahern, A., Wrobel, W., Davidovits, P., Olfert, J., Dubey, M. K., Mazzoleni, C., and Fahey, D. W.: The detection efficiency of the single particle soot photometer, Aerosol Sci. Tech., 44, 612–628, 2010. 5225

Seinfeld, J.: Atmospheric science – black carbon and brown clouds, Nat. Geosci., 1, 15–16, 2008. 5225

Title Page

Abstract | Introduction

Conclusions | References

Tables | Figures

◄ | ►

◄ | ►

Back | Close

Full Screen / Esc

Printer-friendly Version

Interactive Discussion

Table 1. Summary of particle beam width measurements.

Particle Type	Beam Width σ (mm)	Reference
Flame Soot	0.77	(Huffman et al., 2005)
Ambient rBC (roadside, Toronto)	0.46 ± 0.03	this work
300 nm Regal Black	0.40 ± 0.08	this work
200 nm Regal Black	0.39 ± 0.04	this work
Ambient rBC (non-roadside, Toronto)	0.26 ± 0.04	this work
300 nm Nitrate (tungsten vapourizer)	0.22 ± 0.05	this work
Coated Regal Black (UofT, 150 nm core[a])	0.23 ± 0.08	this work
Coated Regal Black (ARI, 300 nm core[b])	0.11 ± 0.03	this work
230 nm DOS	0.12	(Huffman et al., 2005)
Laser Vapourizer (upper limit)	≤ 0.18[c]	this work

[a] $R_{Org/RB} \sim 3$, coated $d_{va} = 280$ nm

[b] $R_{Org/RB} \sim 3$, coated $d_{va} \geq 375$ nm

[c] Derived from BWP attenuation with the probe parallel to laser beam axis, all other measurements were made with a perpendicular BWP orientation.

Title Page

Abstract | Introduction

Conclusions | References

Tables | Figures

◄ | ►

◄ | ►

Back | Close

Full Screen / Esc

Printer-friendly Version

Interactive Discussion
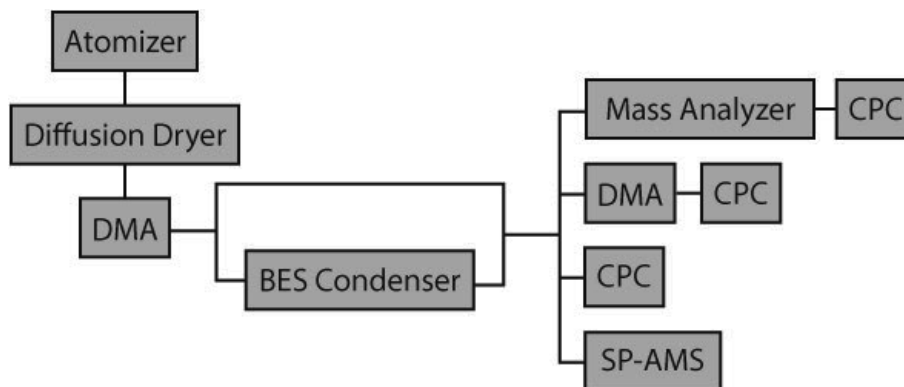
Figure 1. Laboratory schematic showing the basic particle generation, coating and character-ization components. Experiments were conducted independently at the University of Toronto (UofT) and Aerodyne Research, Inc. (ARI) with similar set-ups, see text for details.
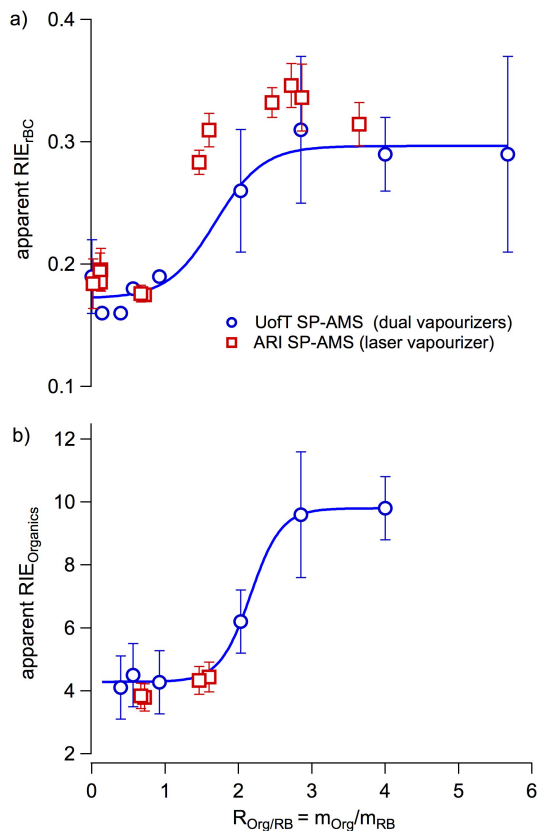
Figure 2. (a) $RIE_{rBC, app}$ measured as a function of BES coating thickness, demonstrating an increase in sensitivity that reaches saturation at approximately $R_{Org/RB} = 3$. Data from two instruments is included: UoT (circles) and ARI data with the laser vapourizer only (squares, SN 215-130). **(b)** $RIE_{Org, app}$ measured as a function of BES coating thickness, demonstrating a similar increase with coating thickness. Error bars represent the standard deviation of 2 to 3 measurements. The blue solid lines represent a best fit to the UoT SP-AMS data.
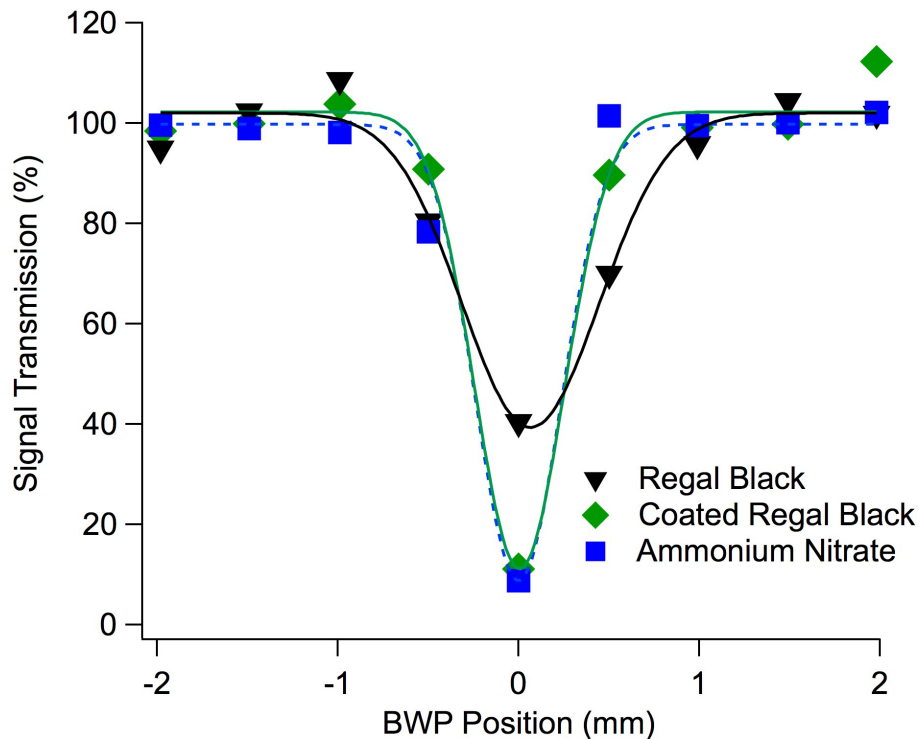
Figure 3. Comparison of BWP signal transmission (signal intensity relative to that of an unblocked beam, normalized to particle number concentration) traces for 200 nm bare ($f_{RB} = 1$), BES coated ($R_{Org/RB} = 3$) Regal Black and 300 nm ammonium nitrate particles vapourized using the tungsten vapourizer as an example of a well focused beam. Data from the UofT SP-AMS.
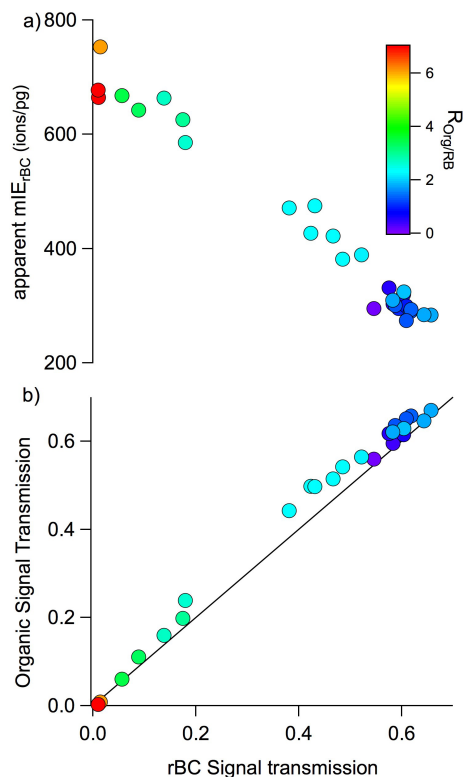
Figure 4. (a) $mIE_{rBC, app}$ as a function of signal transmission with the beam width probe wire at the center of the particle beam. Colours indicate organic coating thickness estimated from SP-AMS measurements of rBC and NR-PM. **(b)** Organic and rBC signal transmission with a 0.41 mm BWP wire at the center of the particle beam, as a function of BES coating thickness ($R_{Org/RB}$). The solid line represents a 1 : 1 relationship. Data from the ARI SP-AMS (SN 215-039).
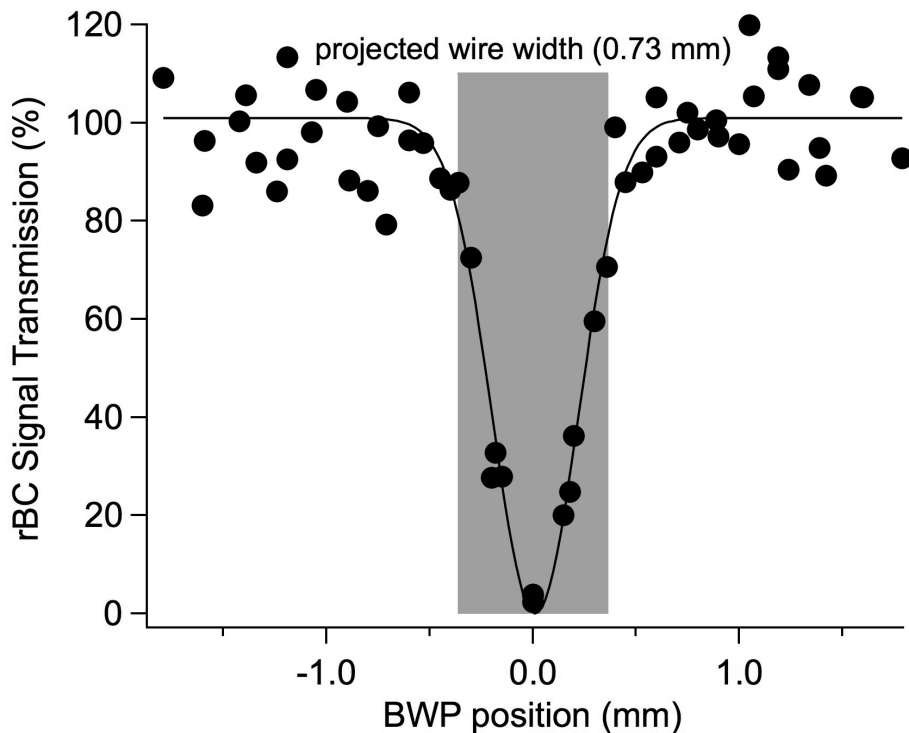
Figure 5. rBC signal transmission as a function of BWP position parallel to the laser beam axis of the SP-AMS. When the 0.46 mm BWP wire was placed in the center of the particle beam, an average of $3 \pm 2\%$ signal transmission was observed indicating that the effective beam width (4σ) is less than the projected width of the wire on the laser vapourizer (shaded region). This corresponds to a beam width (σ) ≤ 0.18 mm. Data from the UofT SP-AMS using uncoated 300 nm (d_m) Regal Black particles.
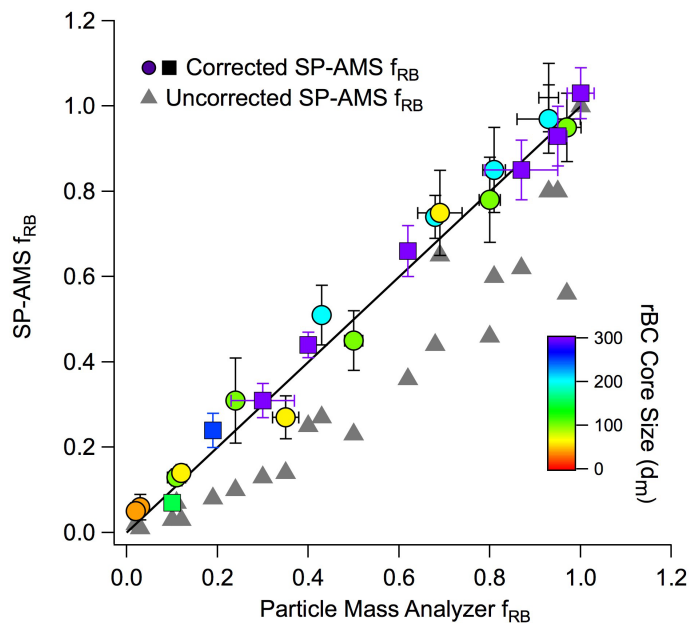
Figure 6. The fraction of Regal Black in BES coated particles (f_{RB}), obtained from particle mass measurements, plotted against the fraction of Regal Black obtained from SP-AMS mass loadings using uncorrected RIE_{rBC} (0.2) and RIE_{Org} (1.4) values (triangles) and RIE values corrected using the relationship observed in Fig. 2. Square points refer to RIE data shown in Fig. 2 that were used to determine the appropriate RIE_{app} values to apply to data from separate experiments at various rBC core sizes (circles). A best-fit line to the data using corrected RIE values yields a slope of 1.01 ± 0.05 with $R^2 = 0.98$. The solid line represents a one-to-one relationship. Data from the UofT SP-AMS. Analogous plots for two ARI SP-AMS instruments are shown in Fig. S3.